A wearable gait analysis system using inertial sensors Part I: Evaluation of measures of gait symmetry and normality against 3D kinematic data

A. Sant'Anna[1], N. Wickström[1] R. Zügner[2] and R. Tranberg[2]
[1]*Intelligent Systems Lab, Halmstad University, Sweden*
[2]*Department of Orthopedics, Sahlgrenska Academy, University of Gothenburg, Sweden*
anita.santanna@hh.se

Keywords: Gait Analysis, Inertial Sensors, Symmetry, Normality

Abstract: Gait analysis (GA) is an important tool in the assessment of several physical and cognitive conditions. The lack of simple and economically viable quantitative GA systems has hindered the routine clinical use of GA in many areas. As a result, patients may be receiving sub-optimal treatment. The present study introduces and evaluates measures of gait symmetry and gait normality calculated from inertial sensor data. These indices support the creation of mobile, cheap and easy to use quantitative GA systems. The proposed method was compared to measures of symmetry and normality derived from 3D kinematic data. Results show that the proposed method is well correlated to the kinematic analysis in both symmetry ($r=0.84$, $p<0.0001$) and normality ($r=0.81$, $p<0.0001$). In addition, the proposed indices can be used to classify normal from abnormal gait.

1 INTRODUCTION

Quantitative gait analysis (GA) can improve the assessment of a number of physical and cognitive conditions. The importance of GA in the treatment of children with cerebral palsy is well known and documented, e.g. (Chang et al., 2010), (DeLuca et al., 1997). The use of GA to monitor and assess Parkinson's Disease, e.g. (Salarian et al., 2004), (Frenkel-Toledo et al., 2005), and stroke, e.g. (Cruz et al., 2008), (Silver et al., 2000), have also been investigated. Changes in gait speed, gait variability, and neurologic gait abnormalities have been associated with the risk of developing dementia and mild cognitive impairment, e.g. (Beauchet et al., 2008), (Verghese et al., 2002).

Although the usefulness of GA is recognized by the medical community, e.g. (Chang et al., 2010), routine clinical use of GA is still not a reality. This is likely due to the costs involved in performing a full 3D GA at a gait lab. As a result of not undergoing GA, many patients may receive sub-optimal treatment, e.g. (Kay et al., 2000), (Lofterød and Terjesen, 2008).

The simpler alternative to in-lab 3D GA is observational GA (OGA), such as the Gillette Functional Assessment Questionnaire (GFAQ) Walking Scale (Novacheck et al., 2000) and the Edinburgh Gait Score (Read et al., 2003). Although some OGA methods have been shown valid and reliable, it is generally understood that they are specific to patient groups, subjective, and sensitive to the observer's experience (Toro et al., 2003). In 1999, Coutts (Coutts, 1999) argued that despite its limitations, OGA would never be totally replaced as the default GA method in the clinical environment because of ease of use. Current technological advancements, however, should encourage clinicians to re-evaluate instrumented GA.

The goal of the present study is to develop a mobile, cheap, and easy to use GA system that quantitatively evaluates certain characteristics of gait independent of location and/or infrastructure. Such a system may be complementary to 3D GA, by providing continuous or frequent monitoring. Alternatively, it may be used where 3D GA is not available such as in underprivileged areas or at home. The system may also be coupled to OGA, providing consistent and reliable quantitative data to aid clinical evaluation.

The proposed method uses accelerometer and gyroscope data to derive measures of gait symmetry and gait normality. The signal analysis is based on the symbolic approach presented in (Sant'Anna and Wickström, 2010), and (Sant'Anna et al., 2011). 19 healthy subjects were measured simultaneously with inertial sensors and a 3D motion capture (MOCAP) system while walking in different ways. Results from the inertial system are compared to measures of symmetry and normality derived from 3D kinematic data.

2 RELATED WORK

2.1 Symmetry

Symmetry refers to the similarity between the movements of the right and left sides of the body. Generally speaking, gait symmetry can be computed from discrete values, e.g. spatio-temporal parameters; or from continuous signals, e.g. joint angles. Some authors have argued that discrete values are not always sufficient to describe gait asymmetry, and that it is important to take into account continuous motion data (Crenshaw and Richards, 2006). It is also important to distinguish between different sources of data. In the present study we will focus on kinematic data extracted from a MOCAP system; and accelerometer and gyroscope data obtained via wearable sensors.

Some approaches to calculating symmetry using continuous accelerometer data have been introduced. (Moe-Nilssen and Helbostad, 2004), for example, introduced an unbiased autocorrelation method using trunk acceleration data. Although this may provide a good general estimate of gait symmetry, it lacks information about each individual limb. More recently (Gouwanda and Senanayake, 2011) used gyroscopes on shanks and thighs to calculate symmetry using a normalized cross correlation approach and the normalized mean error between curves derived from right and left sides. This method segments and normalizes the data to individual strides. As a result, only the shape of the signal and not its relative temporal characteristics are taken into account. Sant'Anna et al. also suggested a symbolic method for estimating gait symmetry using accelerometers (Sant'Anna and Wickström, 2010) or gyroscopes (Sant'Anna et al., 2011), which takes into account not only the shape but also the temporal characteristics of the signal.

Kinematic gait data is usually evaluated by visual inspection of superimposed curves from right and left sides. Few symmetry measures have been proposed which take into account complete joint angle curves. (Crenshaw and Richards, 2006) calculated a measure of trend symmetry based on the variance around the 1st principal component of a right-side vs. left-side plot. This trend symmetry measure is insensitive to scaling, and an additional measure, the range amplitude ratio, is required. The present study introduces a symmetry measure based on kinematic data which can be expressed as one index.

2.2 Normality

Normality refers to the similarity between the movements of one individual compared to average movements of a population that is judged healthy/normal. The Gillette Functional Assessment Questionnaire (GFAQ) Walking Scale is a widely accepted gait normality measure based on observation. Considerable efforts have been put into deriving a similar measure from kinematic data. (Schutte et al., 2000) used principal component analysis (PCA) on 16 discrete normal gait variables to create a representation of the data in a different space. The magnitude of the projection of an abnormal data set onto this space is used as a normality index, known as the Gillette Gait Index (GGI). (Shin et al., 2010) used the same PCA approach to create three separate indices using variables related to ankle, knee and hip kinematics.

A very similar PCA approach, the Gait Deviation Index (GDI), was introduced by (Schwartz and Rozumalski, 2008) using complete joint angle curves. This index showed high correlation with GGI, and distinguished between different levels of the GFAQ. One advantage of PCA approaches is that they transform the possibly dependent gait variables into a new set of independent variables. The disadvantage is that results cannot be traced back to the original gait variables.

(Barton et al., 2007) used self organizing maps (SOM) to create a single representation from many kinetic and kinematic curves. This representation is then used to calculate a measure of distance between abnormal and normal data sets. This approach was later developed into a user friendly graphical user interface that provides a deviation curve for each subject (Barton et al., 2010). The mean value of this deviation curve was highly correlated with the GDI and showed significant difference between different levels of the GFAQ. The difficulty in using this method derives from the fact that large amounts of normal reference data are needed to train the SOM.

A much simpler method, the Gait Profile Score (GPS) and Movement Analysis Profile (MAP), was introduced by (Baker et al., 2009). The MAP is created by taking the root mean square error (RMS) between a reference joint angle curve and the corresponding curve from a subject. This creates one normality index for each joint angle curve. A unique index, the GPI, can be derived by concatenating all joint angle curves end to end, and taking the RMS of this aggregated curve. This work concluded that the GPI and GDI are alternative and closely related measures. Although GDI presents some nice properties such as normal distributions across GFAQ levels, GPS is more easily interpreted because the original variables suffer no transformations and results are given in degrees. (Beynon et al., 2010) also concluded that GPS is significantly correlated with clinical judgment.

No normality indices based on accelerometer or

gyroscope data were found in the literature.

3 METHOD

3.1 Data collection

A group of 19 healthy individuals willing to participate in the experiment were randomly selected. The average hight of the group was 172.1 $\pm$ 7.6 cm; and the average weight was 71.8 $\pm$ 17.2 Kg. Seven participants were male and twelve female, averaging an age of 34 $\pm$ 13 years.

Kinematic and kinetic data were recorded with a 3D motion capture (MOCAP) system, Qualisys MCU 240, sampling at 240Hz. A total of 15 spherical reflective markers, of 19 mm in diameter, were attached to the skin with double-sided tape. Markers were placed on the sacrum, anterior superior iliac spine, lateral knee-joint line, proximal to the superior border of the patella, tibial tubercle, heel, lateral malleolus and between the second and third metatarsals (Tranberg et al., 2011).

Subjects were also equipped with 3 Shimmer® sensor nodes containing one 3-axis accelerometer and one 3-axis gyroscope, sampling at 128Hz. The sensor nodes were attached to the skin with double-sided tape. One node was placed on each outer shank, about 3cm above the lateral malleolus marker, Figure 1(a). The remaining node was placed mid-way between the anterior superior iliac spine markers, Figure 1(b). In addition, one reflective marker was also placed on each sensor node.

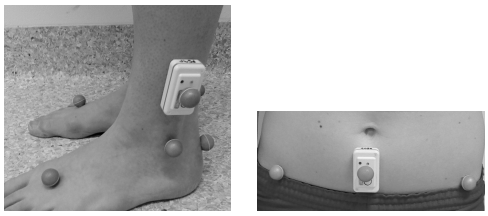

(a) **Shank sensor node** (b) **Waist sensor node**

Figure 1: **Placement of sensor nodes**. Shank sensor node approximately 3cm above the lateral malleolus reflective marker, and waist sensor node mid-way between the anterior superior iliac spine reflective markers.

Before starting the measurements, each sensor node received a beacon signal from a host computer with the host global time in milliseconds since epoch. At this moment, each node stored in its memory card its own local time in milliseconds since epoch together with the host global time. These records were later used to synchronize the sensor data. The data from the sensors is stored in the node.

The subjects were then asked to enter into the measurement volume and a static reference recording was obtained with the Mocap system while the subjects were standing in an upright position aligned with the x-axis of the global coordinate system. Prior to recording, all subjects had the possibility to get familiarized with the walkway and define a comfortable walking speed. The following instructions were then given to the subjects: 1) walk normally at a comfortable speed; 2) walk with a limp, as if injured; and 3) walk slowly, as if tired or pretending to be old. All subjects performed three tests for each type of walk. One test of each type was then randomly chosen for further analysis.

This study was approved by the Regional Ethics Board in Gothenburg, Sweden.

3.2 MOCAP Normality Measure

The normality index used for the kinematic data was the GPS and the MAP (Baker et al., 2009). However, the mean value was removed from all curves before calculating the score, and foot progression was not used because it was not available in the reference data set. Removing the curves' mean values makes the normalcy measure more robust to offset errors, while preserving the shape and range of the curves.

The reference data set is an ensemble of 34 randomly selected adult subjects presenting no known pathologies, previously acquired at the clinical gait lab at Sahlgrenska University Hospital, Gothenburg, Sweden. Joint angle curves were calculated for each individual and normalized to stride time. The ensemble average of the normalized curves was used as a reference curve.

Each MAP component was calculated as the RMS difference, $MAP = \sqrt{\frac{1}{N}\sum_{n=1}^{N}(C_{subj}(n) - C_{ref}(n))^2}$, between the reference curve, C_{ref}, and the subject's curve, C_{subj}, Figure 2, where N is the number of points in the curve. The GPS was calculated similarly by concatenating all joint curves end to end.

For each subject, MAP and GPS results were calculated as the average between right side and left side MAP and GPS respectively.

3.3 MOCAP Symmetry Measure

Based on the GPS, a measure of symmetry was derived for the kinematic data. In this case, the components of MAP-symmetry were calculated as the RMS error between the curves for the right and left sides, after removing their corresponding mean values. Similarly, GPS-symmetry was calculated by concatenating all joint curves end to end and calculating the

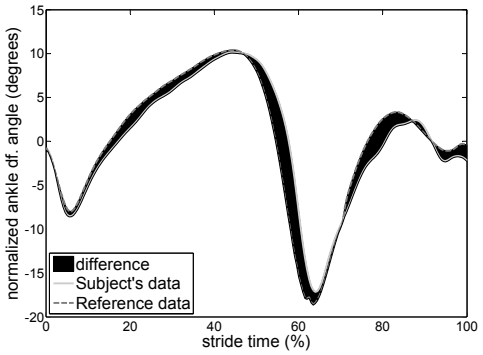

Figure 2: **Calculating the MAP**. The MAP for this joint angle progression is calculated as the RMS of the difference between the subject's curve and the reference curve, i.e. the RMS of the shaded area.

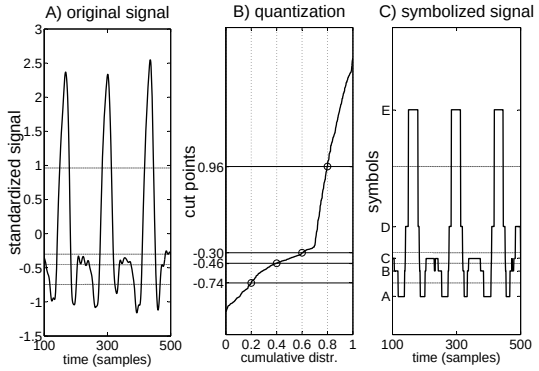

Figure 3: **Symbolization**. In this example, the signal was symbolized into 5 symbols. (A) shows the original signal after standardization. (B) shows the empirical cumulative distribution of the signal, probability levels are shown on the horizontal axis. The quantization levels, cut points, are the values at which the probability of the signal increases by $1/Number_{symbols} = 1/5 = 0.2$. (C) illustrates the corresponding symbolized signal. Note that the probability of each symbol occurring in the symbolized signal is 20%.

RMS difference between left and right sides.

3.4 Inertial Sensor Symmetry Measure

The symmetry measure used in this paper was presented in (Sant'Anna and Wickström, 2010) and also used in (Sant'Anna et al., 2011), with a different symbolization technique. The sensor signal, accelerometer or gyroscope, is standardized to zero mean and unitary standard deviation, then segmented into N symbols. Symbolization is done by quantization into N levels. The quantization levels are chosen based on the empirical probability distribution of the signal, so as to produce equiprobable symbols, Figure 3.

The period between consecutive occurrences of the same symbol are calculated and stored in a period histogram (Sant'Anna et al., 2011). Similarly, the period between consecutive transitions from symbol i to symbol j are calculated and stored in a transition histogram. The symmetry index is a measure of the similarity between symbol (transition) period histograms for the right and left sides. Histograms are compared using a relative error measure shown in Eq. 1, where Z is the number of symbols; K is the number of bins in the histograms; n_i is the number of non-empty histogram bins (for either foot) for symbol i; $h_{Ri}(k)$ is the normalized value for bin k in the period histogram i for the *right* foot; and $h_{Li}(k)$ is the normalized value for bin k in the period histogram i for the *left* foot.

$$SI_{symb} = \frac{\sum_{i=1}^{Z} \frac{1}{n_i} \sum_{k=1}^{K} |h_{Ri}(k) - h_{Li}(k)|}{\sum_{i=1}^{Z} \frac{1}{n_i} \sum_{k=1}^{K} |h_{Ri}(k) + h_{Li}(k)|} 100 \qquad (1)$$

3.5 Inertial Sensor Normality Measure

The normality measure for the inertial sensor data was derived from the symmetry measure, Part 3.4. Instead of comparing the histograms for right and left sides, one subject's histograms are compared to histograms derived from a reference data set. The reference data set was formed by selecting the subjects that presented the smallest GPS based on the normal walk kinematic data.

The normal walk inertial sensor data from these reference subjects was standardized to zero mean and unitary standard deviation, symbolized, and symbol (transition) periods were calculated. The symbol (transition) periods were normalized to stride time. That is, a period that coincides with stride time is represented as 1 and all other periods are scaled correspondingly. This normalization is common when dealing with kinematic data, and it ensures that the analysis is not affected by gait speed. The symbol (transition) periods from all reference subjects were used to create reference histograms.

Reference histograms were compared to the histograms from right and left sides of each subject, Eq. 2, where h_{ref} are the reference histograms and h_{subj} are the subject histograms. Right and left results were averaged to create the normality measure for the subject.

$$NORM_{symb} = \frac{\sum_{i=1}^{Z} \frac{1}{n_i} \sum_{k=1}^{K} |h_{ref}(k) - h_{subj}(k)|}{\sum_{i=1}^{Z} \frac{1}{n_i} \sum_{k=1}^{K} |h_{ref}(k) + h_{subj}(k)|} 100 \qquad (2)$$

3.6 Stride Time Estimation

The period (transition) histograms can also be used to estimate gait events (Sant'Anna and Wickström,

2010). In the present study, stride time was calculated by first determining which of the symbols (transitions) presented periods with standard deviations smaller or equal to 1/5 of their mean value. This rule identifies the symbols (transitions) that occur regularly in every cycle. The mean period of the highest symbol (transition) was used as an estimate of the stride time. The highest symbol (transition) was chosen based on a priori knowledge that the gyroscope data presents a prominent spike at mid-swing (Salarian et al., 2004), and the accelerometer data presents a prominent spike at heel-strike (Aminian et al., 1999). As described in (Sant'Anna and Wickström, 2010), a priori expert knowledge can be used to identify gait events in the signal, from which various temporal parameters may be derived, e.g. double-support time.

3.7 Analysis

The data acquired from the MOCAP system was processed in Visual 3D (C-Motion Inc., Germantown, MD) to generate kinematic join angle data and spatio-temporal parameters such as stride time. The data was then exported to MATLAB (MathWorks, Natick, MA) where MAP, GPS and MOCAP symmetry were calculated for each subject and used as reference.

The signals from the shank accelerometers and gyroscopes were low-pass filtered with a Butterworth filter of order 6 and cut-off frequency 20Hz. The waist sensor data was filtered at 10Hz. The signals were filtered once, then reversed and filtered again to avoid any phase shift. The three axes of each accelerometer were combined into a resultant signal, $A_{res} = \sqrt{A_x^2 + A_y^2 + A_z^2}$. For each gyroscope, only pitch and roll rotations were considered, $G_{res} = \sqrt{G_{pitch}^2 + G_{roll}^2}$.

Symmetry and stride times were calculated using right and left shank signals. Normality was calculated using both shanks and waist signals. Measures were calculated considering both period histograms and transition histograms, varying from 5 to 25 symbols. The resulting values outside two standard deviations were considered outliers and removed. The remaining values were used to calculate the Spearman's rank correlation coefficient with reference measurements. The optimal number of symbols and the choice of histogram were chosen so as to maximize the correlation coefficients. A two-sample t-test was used to determine if the final normality and symmetry values distinguish between normal and other walks. All hypothesis were bi-directional with confidence level, $\alpha = 0.05$. All sensor data analysis was undertaken in MATLAB.

4 RESULTS

Some of the data was excluded due marker obstruction or sensor failure. The total number of subjects used for each analysis is shown in Table 1.

Table 1: Number of subjects available for analysis

walk	placement	accelerometer	gyroscope
Normal	shank	16	14
	waist	16	15
Slow	shank	13	12
	waist	13	12
Limp	shank	16	14
	waist	16	15

An example of the shank sensor node data and corresponding symbolized data is shown in Figure 4.

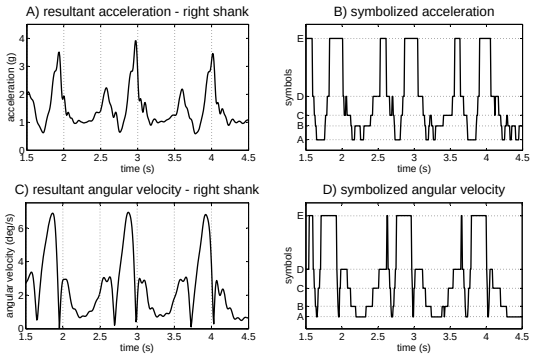

Figure 4: **Example shank inertial sensor data**. (A) illustrates a typical resultant acceleration signal from a shank sensor. (B) exemplifies the symbolization of the acceleration signal using 5 symbols. (C) illustrates a typical gyroscope resultant signal acquired with the same sensor as (A). (D) exemplifies the symbolized gyroscope signal using 5 symbols. Signals (A) and (C) come from a normal walk trial and are synchronized in time.

Figure 5 shows the MAP and GPS results for all subjects during normal walking and limp walking. There is a significant difference between the different walks. The overall amplitude of the scores is reduced by approximately a factor of 2 compared to results presented (Baker et al., 2009). This is caused by the absence of curves' mean values. Another contributing factor is that the present work considers healthy adults instead of children.

The best normality results using the shank sensors were obtained with the accelerometer data, 5 symbols, and symbol period histograms. Statistically significant Spearman's rank correlation coefficients are shown in Table 2. Note that the normality measure derived from the shank sensor correlates better with ankle, knee and hip flexion MAP components than with the other MAP components. The combination of all MAP components into the GPS, however, correlates better than most individual components, with the

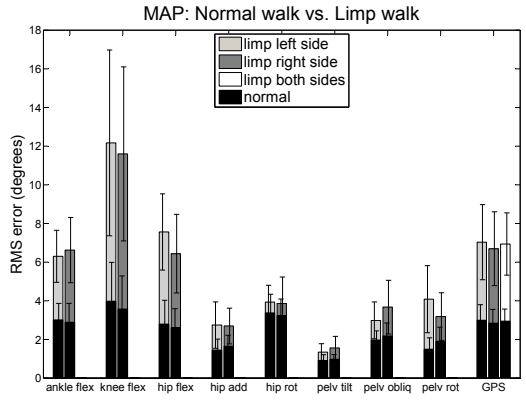

Figure 5: **MOCAP normality**. MAP and GPS results for the limp data set are shown against the normal data set results.

Table 2: Correlation of normality measures - shank.

sensor	accelerometer	
placement	shank	
histogram	symbol period	
no. symbols	5	
variable	r	p-value
MAP ankle flex.	0.58	<0.0001
MAP knee flex.	0.73	<0.0001
MAP hip flex.	0.78	<0.0001
MAP pelv. obliq.	0.44	< 0.0001
MAP pelv. rot.	0.49	< 0.0001
GPS	0.74	< 0.0001

exception of hip flexion. The normality index derived from the accelerometer placed on the waist correlated with the MOCAP reference better than the shank sensor data, Table 3. The optimal combination in this case was 18 symbols and transition histograms.

The best correlation of the inertial sensor symmetry with the reference was achieved with the shank gyroscopes, 20 symbols, and symbol period histograms. The best correlation coefficients are shown in Table 4. Once again, the measure derived from the shank sensor correlates better with ankle, knee and hip flexion MAP components.

Stride time derived from the symbolized data were accurate. The correlation with the reference data was 0.97, $p<0.0001$. After eliminating 2 outliers, the total RMS error was 0.048 seconds. The best stride time results were achieved using 17 symbols and transition histograms.

Figures 6 and 7 show the symmetry and normality results respectively. Two-sample t-tests indicated that the MOCAP symmetry data for normal walk was significantly different from limp, $p<0.0001$, and slow walk, $p=0.03$. The gyroscope symmetry index was also significantly different between normal and limp, $p<0.0001$, and normal and slow, $p=0.02$, data sets. Similarly, normality indices were all significantly different between data sets, $p<0.0001$.

Table 3: Correlation of normality measures - waist.

sensor	accelerometer	
placement	waist	
histogram	transition	
no. symbols	18	
variable	r	p-value
MAP ankle flex.	0.69	<0.0001
MAP knee flex.	0.77	<0.0001
MAP hip flex.	0.82	<0.0001
MAP hip add.	0.47	<0.0001
MAP pelv. obliq.	0.49	<0.0001
MAP pelv. rot.	0.71	< 0.0001
GPS	0.81	< 0.0001

Table 4: Correlation of symmetry measures - shank.

sensor	gyroscope	
placement	shank	
histogram	symbol period	
no. symbols	20	
variable	r	p-value
ankle flex.	0.64	< 0.0001
knee flex.	0.81	< 0.0001
hip flex.	0.68	< 0.0001
all	0.84	< 0.0001

5 DISCUSSION

It is important to stress that the MOCAP system and the inertial sensors measure very different things. Nonetheless, the raw data from both system can be processed in order to determine certain properties or characteristics of gait which are the same or comparable. The MAP components, for example, convey the normality of very specific joint movements. The normality measure derived from the sensors, on the other hand, expresses an overall normality of the shank movements, which are caused by a combination of different joint movements. The comparison of the sensor normality with the different MAP components, however, may provide insight into the the factors that influence the sensor normality measure.

Although the shank sensor normality correlates well with hip flexion and not with pelvic rotation, the waist sensor normality correlates well with both. This suggests that the shank sensors are mostly affected by the abnormalities in hip flexion, whereas the waist sensor is affected by abnormalities in hip flexion and pelvic rotation. This is aligned with the fact most gait pathologies affect the movement of the center of gravity (Detrembleur et al., 2000), which is captured by the waist sensor.

Another interesting factor is that the correlation of sensor symmetry with the MOCAP symmetry considering all components, is greater than the correlation with any individual component. This may suggest that the symmetry of individual joint angles is not representative of the symmetry of the movement as a whole, or at least not representative of the movement of the shanks. It is the combination of joint movements that results in the overall symmetry captured by the shank sensors.

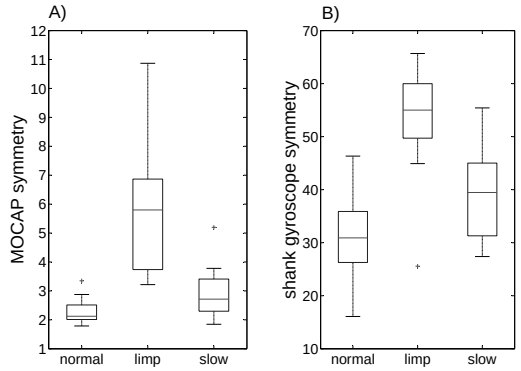

Figure 6: **Symmetry indices**. Distributions are presented as boxplots. (A) illustrates the MOCAP symmetry results for normal, limp and slow data sets. Results for the normal data set were significantly different from limp ($p<0.0001$) and slow ($p=0.03$) data sets. (B) shows the shank gyroscope symmetry index, using 20 symbols and period histograms. The symmetry of the normal data set was significantly different to that of limp ($p<0.0001$) and slow ($p=0.02$) data sets.

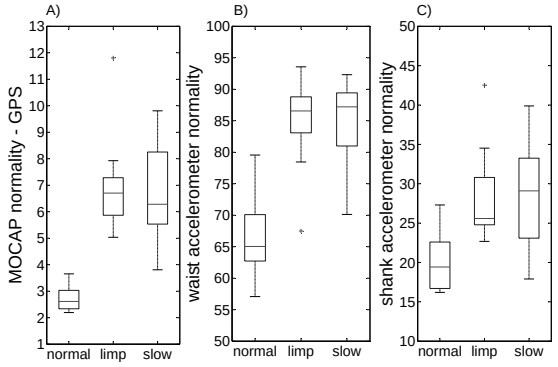

Figure 7: **Normality indices**. Distributions are presented as boxplots. (A) shows the GPS for all three types of walk. Normal and limp, and normal and slow data sets were significantly different ($p<0.0001$). (B) illustrates the normality results of all types of walk using the waist accelerometer, 18 symbols, and transition histograms. Data sets were significantly different ($p<0.0001$). (C) shows results of the normality index using shank accelerometers, 5 symbols, and symbol period histograms. Similarly, normal walk was significantly different from limp and slow data sets ($p<0.0001$).

One may argue that the lack of information about individual joint movements or other particular kinematic and kinetic parameters diminishes the usefulness of the proposed method. However, the symbolic representation, once it is properly understood, may reveal more precise information about the movement. Consider for example the signals shown in Figure 8. (A) illustrates the gyroscope resultant signal after symbolization of a subject walking normally, and

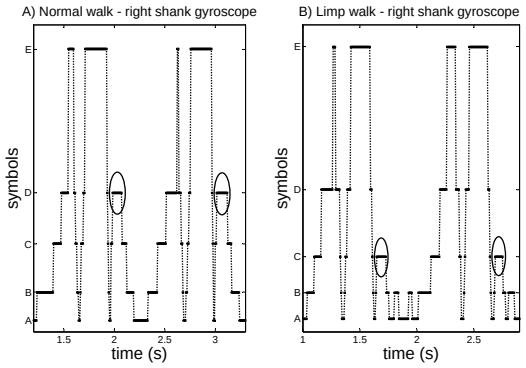

Figure 8: Comparing normal and limp walk. (A) illustrates the gyroscope resultant signal after symbolization of a subject walking normally, and (B) shows the signal from the same sensor when the subject was limping. Only two strides are depicted in each plot. Note how symbol D in the normal signal is replaced by signal C in the limp signal. This exemplifies how the symbolic representation of the signals may be used to derive particular information about the subject's gait pattern.

(B) shows the signal from the same sensor when the subject was limping. Only two strides are depicted in each plot.

Note how symbol D in the normal signal is replaced by signal C in the limp signal. It is known that symbol C represents a lower angular velocity than symbol D. As previously mentioned, it is also known that these symbols occur shortly after heel-strike. Therefore, this difference from normal to limp indicates that the shank rotated more slowly after heel-strike when the subject was limping. Given that the duration of the symbols is approximately the same, the shank rotated to smaller angle. The extraction of such information is not trivial, but expert systems can be developed for this purpose. Another advantage of the proposed instrumented GA is that, after a diagnosis or clinical evaluation has been made, the recovery or progress of the patient can be easily measured according to symmetry and normality.

Results show that the normal walk can be distinguished from the other walks with respect to normality and symmetry. Although limp and slow walk were "acted" and not real, the purpose of the instructions was to generate abnormal gait patterns. The distribution of the GPS shows that the fake patterns ranged over varying levels of abnormality. This variety in the data is useful in evaluating the expressiveness of the proposed method, and how well it covers a wide range of abnormalities. Results suggest that the normality and symmetry measures are gradual and can, in fact, be used to express varying levels of abnormality.

One important observation is that the proposed method utilizes several steps for the analysis. In con-

trast, the MOCAP system is commonly limited to one stride per foot, because only two force plates are available in most gait labs. The acquisition of a larger number of steps greatly increases the amount of work needed. Moreover, one stride may not be representative of a subject's average gait pattern due to intra-subject variability (Chau et al., 2005). The sensor data used in the present study was relatively short, averaging approximately 3 strides at constant speed for normal and limp walk. Longer data recordings might provide more accurate analysis.

When using inertial sensors for human movement analysis, the placement of the sensors can greatly affect results. In the present study, for example, the waist sensor was attached to the front of the subject. Most studies however, attach the sensor to the back, e.g. (Moe-Nilssen and Helbostad, 2004), (Auvinet et al., 1999), (Hartmann et al., 2009). The present study is part of a larger study where hip-replacement patients were being monitored with an inertial sensor node for long periods of time. It was decided that a sensor placed in the front would be more comfortable than one in the back. The gait data collection kept the same configuration. However, for short data collections, dealing with a varied pool of subject, it might be beneficial to place the sensor at the back. This way, the sensor may stay closer to the center of gravity regardless of the weight or shape of the subject.

MOCAP systems and inertial sensor systems should not compete, they should complement each other. MOCAP systems measure the position of sets of reflective skin markers, specific to a marker model that defines the orientation of each body segment. Accelerations, rotations and joint angles are obtained through specific algorithms developed for that particular marker model. One may wonder if the constraints imposed by different models and filters distort the original data. Gait is already a well studied area, but new movements require new models. Inertial sensors such as accelerometers and gyroscopes may contribute to the study of movements that are not yet fully understood, e.g. freezing of gait in Parkinson's Disease patients (Plotnik et al., 2005), (Hausdorff et al., 2003). They also complement MOCAP systems in that they are mobile, and can be used in a wider variety of contexts.

6 CONCLUSION

This study presented and evaluated a method for gait analysis using inertial sensor data. A novel method for measuring gait normality was introduced, based on a symbolic approach previously used for gait symmetry. Symmetry and normality results were compared to a reference derived from kinematic data. Results support that an estimate of gait symmetry and normality, related to that derived from MOCAP data, can be obtained with a simple combination of inertial sensors. This supports the development of a cheap and easy to use system for quantitative gait analysis that can be used both in the clinic and in other less controlled environments.

The proposed measures of symmetry and normality correlate well with the reference GPS and symmetry MOCAP measures. A follow-up study on hip-replacement patients will attempt to determine if the proposed method is also in agreement with clinical judgment. This expectation is supported by the fact that GPS is, in turn, well correlated with clinical judgment.

ACKNOWLEDGMENTS

This study was partially funded by the Promobilia Foundation and the Institute of Health and Care Sciences, Sahlgrenska Academy, University of Gothenburg, Sweden.

REFERENCES

Aminian, K., Rezakhanlou, K., De Andres, E., Fritsch, C., Leyvraz, P. F., and Robert, P. (1999). Temporal feature estimation during walking using miniature accelerometers: an analysis of gait improvement after hip arthroplasty. *Medical and Biological Engineering and Computing*, 37:686–691.

Auvinet, B., Chaleil, D., and Barrey, E. (1999). Accelerometric gait analysis for use in hospital outpatients. *Revue du Rhumatisme: English ed.*, 66(7-9):389–397.

Baker, R., McGinley, J. L., Schwartz, M. H., Beynon, S., Rozumalski, A., Graham, H. K., and Tirosh, O. (2009). The gait profile score and movement analysis profile. *Gait & Posture*, 30(3):265–269.

Barton, G., Lisboa, P., Lees, A., and Attfield, S. (2007). Gait quality assessment using self-organising artificial neural networks. *Gait & Posture*, 25(3):374 – 379.

Barton, G. J., Hawken, M. B., Scott, M. A., and Schwartz, M. H. (2010). Movement deviation profile: A measure of distance from normality using a self-organizing neural network. *Human Movement Science*, In Press, Corrected Proof.

Beauchet, O., Allali, G., Berrut, G., Hommet, C., Dubost, V., and Assal, F. (2008). Gait analysis in demented subjects: interests and perspectives. *Neuropsychiatric Disease and Treatment*, 4(1):155–160.

Beynon, S., McGinley, J. L., Dobson, F., and Baker, R. (2010). Correlations of the gait profile score and the

movement analysis profile relative to clinical judgments. *Gait & Posture*, 32(1):129–132.

Chang, F. M., Rhodes, J. T., Flynn, K. M., and Carollo, J. J. (2010). The role of gait analysis in treating gait abnormalities in cerebral palsy. *Orthopedic Clinics of North America*, 41(4):489 – 506.

Chau, T., Young, S., and Redekop, S. (2005). Managing variability in the summary and comparison of gait data. *Journal of NeuroEngineering and Rehabilitation*, 2(1):22.

Coutts, F. (1999). Gait analysis in the therapeutic environment. *Manual Therapy*, 4(1):2 – 10.

Crenshaw, S. J. and Richards, J. G. (2006). A method for analyzing joint symmetry and normalcy, with an application to analyzing gait. *Gait & Posture*, 24(4):515 – 521.

Cruz, H. et al. (2008). Evidence of abnormal lower-limb torque coupling after stroke: An isometric study supplemental materials and methods. *Stroke*, 39(1):139.

DeLuca, P. A., Davis, R. B., unpuu, S., Rose, S., and Sirkin, R. (1997). Alterations in surgical decision making in patients with cerebral palsy based on three-dimensional gait analysis. *Journal of Pediatric Orthopaedics*, 17(5):608–614.

Detrembleur, C., van den Hecke, A., and Dierick, F. (2000). Motion of the body centre of gravity as a summary indicator of the mechanics of human pathological gait. *Gait & Posture*, 12(3):243–250.

Frenkel-Toledo, S., Giladi, N., Peretz, C., Herman, T., Gruendlinger, L., and Hausdorff, J. (2005). Effect of gait speed on gait rhythmicity in Parkinson's disease: variability of stride time and swing time respond differently. *Journal of NeuroEngineering and Rehabilitation*, 2(1):23.

Gouwanda, D. and Senanayake, A. S. M. N. (2011). Identifying gait asymmetry using gyroscopes–a cross-correlation and normalized symmetry index approach. *Journal of Biomechanics*, 44(5):972 – 978.

Hartmann, A., Murer, K., de Bie, R., and de Bruin, E. D. (2009). Reproducibility of spatio-temporal gait parameters under different conditions in older adults using a trunk tri-axial accelerometer system. *Gait & Posture*, 30(3):351–355.

Hausdorff, J. M., Schaafsma, J. D., Balash, Y., Bartels, A. L., Gurevich, T., and Giladi, N. (2003). Impaired regulation of stride variability in parkinson's disease subjects with freezing of gait. *Experimental Brain Research*, 149:187–194.

Kay, R. M., Dennis, S., Rethlefsen, S., Reynolds, R. K., Skaggs, D. L., and Tolo, V. T. (2000). The effect of preoperative gait analysis on orthopaedic decision making. *Clinical Orthopaedics and Related Research*, 372:217–222.

Lofterød, B. and Terjesen, T. (2008). Results of treatment when orthopaedic surgeons follow gait-analysis recommendations in children with cp. *Developmental Medicine & Child Neurology*, 50(7):503–509.

Moe-Nilssen, R. and Helbostad, J. L. (2004). Estimation of gait cycle characteristics by trunk accelerometry. *Journal of Biomechanics*, 37(1):121 – 126.

Novacheck, T. F., Stout, J. L., and Tervo, R. (2000). Reliability and validity of the gillette functional assessment questionnaire as an outcome measure in children with walking disabilities. *Journal of Pediatric Orthopaedics*, 20(1):75.

Plotnik, M., Giladi, N., Balash, Y., Peretz, C., and Hausdorff, J. M. (2005). Is freezing of gait in Parkinson's disease related to asymmetric motor function? *Annals of Neurology*, 57(5):656–663.

Read, H. S., Hazlewood, M. E., Hillman, S. J., Prescott, R. J., and Robb, J. E. (2003). Edinburgh visual gait score for use in cerebral palsy. *Journal of Pediatric Orthopaedics*, 23(3):296–301.

Salarian, A., Russmann, H., Vingerhoets, F., Dehollain, C., Blanc, Y., Burkhard, P., and Aminian, K. (2004). Gait assessment in Parkinson's disease: Toward an ambulatory system for long-term monitoring. *IEEE Transactions on Biomedical Engineering*, 51(8):1434 –1443.

Sant'Anna, A., Salarian, A., and Wickström, N. (2011). A new measure of movement symmetry in early parkinson's disease patients using symbolic processing of inertial sensor data. *IEEE Transaction on biomedical Engineering*. Epub ahead of print, 2011.

Sant'Anna, A. and Wickström, N. (2010). A symbol-based approach to gait analysis from acceleration signals: Identification and detection of gait events and a new measure of gait symmetry. *IEEE Transactions on Information Technology in Biomedicine*, 14(5):1180 – 1187.

Schutte, L. M., Narayanan, U., Stout, J. L., Selber, P., Gage, J. R., and Schwartz, M. H. (2000). An index for quantifying deviations from normal gait. *Gait & Posture*, 11(1):25–31.

Schwartz, M. H. and Rozumalski, A. (2008). The gait deviation index: A new comprehensive index of gait pathology. *Gait & Posture*, 28(3):351–357.

Shin, K.-Y., Rim, Y., Kim, Y., Kim, H., Han, J., Choi, C., Lee, K., and Mun, J. (2010). A joint normalcy index to evaluate patients with gait pathologies in the functional aspects of joint mobility. *Journal of Mechanical Science and Technology*, 24:1901–1909.

Silver, K., Macko, R., Forrester, L., Goldberg, A., and Smith, G. (2000). Effects of aerobic treadmill training on gait velocity, cadence, and gait symmetry in chronic hemiparetic stroke: A preliminary report. *Neurorehabilitation and Neural Repair*, 14(1):65–71.

Toro, B., Nester, C., and Farren, P. (2003). A review of observational gait assessment in clinical practice. *Physiotherapy Theory and Practice*, 19(3):137–149.

Tranberg, R., Saari, T., Zügner, R., and Kärrholm, J. (2011). Simultaneous measurements of knee motion using an optical tracking system and radiostereometric analysis (RSA). *Acta Orthopaedica*, 82(2):171–176.

Verghese, J., Lipton, R., Hall, C., Kuslansky, G., Katz, M., and Buschke, H. (2002). Abnormality of gait as a predictor of non-Alzheimer's dementia. *New England Journal of Medicine*, 347(22):1761.